Fuel Processing Technology 262 (2024) 108111

Contents lists available at ScienceDirect

Fuel Processing Technology

journal homepage: www.elsevier.com/locate/fuproc

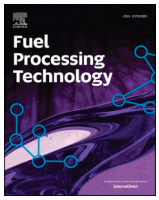

Carbon monoxide (CO) and particulate matter (PM) emissions during the combustion of wood pellets in a small-scale combustion unit – Influence of aluminum-(silicate-)based fuel additivation

Theresa Siegmund *, Christian Gollmer, Niklas Horstmann, Martin Kaltschmitt

Institute of Environmental Technology and Energy Economics, Hamburg University of Technology (TUHH), Eissendorfer Strasse 40, 21073 Hamburg, Germany

ARTICLE INFO

Keywords:
Wood Pellets
Combustion
Total Particulate Matter (TPM) Emissions
(Fuel) Additivation
Carbon Monoxide (CO) Emissions
Kaolin

ABSTRACT

The additivation of solid biofuels has proven to be an effective method for reducing total particulate matter (TPM) and carbon monoxide (CO) emissions, as well as for reducing ash-related problems related to, e.g., fouling and slagging. During the combustion with additives, potassium (K) released from the solid biofuels is bound into temperature-stable compounds, thus preventing the formation of inorganic (i.e., K-based) TPM. Simultaneously by reducing K in the gas phase, the inhibition of gas-phase oxidation (e.g., CO oxidation) due to interference of K within the existing radical pool is hindered. Particularly kaolin, an aluminum-silicate-based additive has proven effective in reducing not only TPM but also CO emissions. The mitigation effects on CO emissions have previously been reported mostly in a subordinate role and explanations are given in the form of hypotheses. In this study, seven additives (i.e., kaolin, kaolinite, meta-kaolinite, aluminum hydroxide, muscovite, muscovite coated with titanium dioxide and kalsilite, each at 0.3 $wt\%_{a.r.}$) were investigated during wood pellet combustion in a small-scale furnace (7.8 kW). For both CO and TPM emissions, kaolin proved to be most effective (i.e., −52% CO, −49% TPM), followed by muscovite, kaolinite, TiO_2 coated muscovite, aluminum hydroxide, and meta-kaolinite.

1. Introduction

In the domestic heating sector small-scale combustion units for wood (i.e., mostly logs and pellets) play a significant role in the provision of renewable heat [1], while releasing emissions harmful to the environment and human health. These emissions originate from inorganic aerosol-forming elements contained naturally within the biomass (e.g., particulate matter (PM) emissions) or from an incomplete combustion (e.g., carbon monoxide (CO) emissions)). These challenges are still not fully addressed.

To comply with the legal limits for PM and CO emissions in small-scale combustion systems defined by law e.g., in Germany (e.g., 30 mg/Nm^3 and 250 mg/Nm^3 for pellet stoves without water pockets [2]), various measures can be taken. These measures can be divided into

- fuel side measures (e.g., fuel pre-treatment or additivation),
- primary measures (i.e., optimizing combustion efficiency e.g., by modifying air-fuel ratio or furnace geometry), and
- secondary measures (e.g., downstream flue gas cleaning).

Especially for small-scale combustion units the first measure, more precisely (solid) fuel additivation, offers high potential to reduce the emission of (inorganic) PM by binding ash- and PM-forming elements (especially potassium (K)) within the ash. As opposed to secondary measures with high capital costs (and for small scale typically not feasible) [3], the additional costs of fuel additivation can be expected to range from 0.1 to 1.0% of the costs of the fuel (prices assumed for the use of 0.3–1 wt% kaolin with wood pellets [4–6]).

Al-, Ca-, Mg- and P-based additives have proven to show a certain reduction potential for TPM (and partially for CO) [7]. Among these, the Al-Si-based additive kaolin, primarily composed of the mineral kaolinite, has been repeatedly identified as being most effective (e.g., [7–12]). During combustion, K contained naturally within a solid biofuel is primarily released in the form of volatile gaseous compounds (e.g., as potassium hydroxide (KOH), potassium chloride (KCl), potassium sulfate (K_2SO_4), potassium carbonate (K_2CO_3)) into the surrounding gas phase [13]. Due to cooling effects in either the stack or the atmosphere, these alkali components undergo nucleation and agglomeration, consequently constituting the predominant part of the released inorganic PM emissions [14]. By adding additives such as kaolin, alkali

* Corresponding author.
E-mail address: theresa.siegmund@tuhh.de (T. Siegmund).

https://doi.org/10.1016/j.fuproc.2024.108111
Received 26 March 2024; Received in revised form 8 July 2024; Accepted 13 July 2024
Available online 31 July 2024

metals such as K are incorporated primarily through chemical reactions into temperature-stable compounds remaining within the bottom ash and thus preventing the formation of TPM emissions [8] (refer to eq. (7)–(10) in section 2).

Some studies have also shown a significant reduction in CO emissions by additivation of solid biofuels with selected additives. This is most widely reported for kaolin (consisting mostly of kaolinite $Al_2Si_2O_5(OH)_4$) resulting in a reduction of up to 90% in the flue gas (e.g., [8,10,11,15,16]). Unlike the well-documented reduction of TPM, there has been limited explanation regarding the mitigation of CO; however, authors have proposed some hypotheses, including the catalytic activity of kaolin (and/or intermediate products) on fuel oxidation or the alteration of fire bed structure due to the formation of K-Al-silicates, which may avoid CO channels and layers [11]. Recent research suggests that the shift of K from the gas phase into solid components in the bottom ash results in reduced K-induced inhabitation effects on CO oxidation due to interference with O/H radicals (i.e., mainly hydroxyl radicals ($^{\bullet}OH$)) [17]. The oxidation of CO in the gas phase is known to occur mostly via the reaction with $^{\bullet}OH$ radicals (eq. (1)) [18].

$$CO + {}^{\bullet}OH \leftrightharpoons CO_2 + H^{\bullet} \quad (1)$$

KCl and KOH in the gas phase may react with $^{\bullet}H$ radicals, forming atomic K and HCl/H_2O (eqs. (2) and (3)). Atomic K may then react with $^{\bullet}OH$ radicals and O_2, forming KOH and $KO_2^{\bullet}$ (eqs. (4) and (5)) from which $KO_2^{\bullet}$ may then react with $^{\bullet}OH$ radicals to form KOH (eq. (6)). This leads to an overall radical removal [19].

$$KOH + H^{\bullet} \leftrightharpoons K^{\bullet} + H_2O \quad (2)$$

$$KCl + H^{\bullet} \leftrightharpoons K^{\bullet} + HCl \quad (3)$$

$$K^{\bullet} + {}^{\bullet}OH + M \leftrightharpoons KOH + M \quad (4)$$

$$K^{\bullet} + O_2 + M \leftrightharpoons KO_2{}^{\bullet} + M \quad (5)$$

$$KO_2{}^{\bullet} + {}^{\bullet}OH \leftrightharpoons KOH + O_2 \quad (6)$$

With K bound in temperature-stable components within the ash, these radical reactions are suppressed, resulting in a higher radical availability and promoting CO and gas phase oxidation.

Against this background, the scope of this paper is to investigate the CO mitigation potentials of (K-)Al-(Si-)based additives, including (intermediate) products of K incorporation. For this, previous research results regarding the CO and TPM emissions during the combustion of solid biofuels in a small-scale combustion furnace (i.e., pellet stove) with well investigated additives were validated and further additives are included. The additives utilized were Al-silicates (i.e., kaolin, kaolinite), aluminum hydroxide, as well as the (intermediate) products of K incorporation (i.e., muscovite (plain and coated with titanium dioxide (TiO_2)), and kalsilite). Additionally, meta-kaolinite was investigated; meta-kaolinite is the dehydrated, amorphous form of kaolinite and essentially the reactive form of the Al-silicate for K incorporation (section 2). For all combustion experiments, the TPM and CO emissions were measured, and the chemical composition of the TPM emissions as well as the residual combustion ash were analyzed.

2. Additive reaction paths

Below, the current state of knowledge for the reactions of the utilized additives with volatile, K-containing compounds from organic matter associated with TPM emission formation and the inhibition of CO/ gas phase oxidation, are discussed.

2.1. Kaolin/Kaolinite ($Al_2Si_2O_5(OH)_4$)

The main constituent and chemically reactive component of kaolin is the clay mineral kaolinite ($Al_2Si_2O_5(OH)_4$), characterized by a layered structure with a large specific surface area and a low porosity [20]. During the combustion process, kaolinite is dehydrated and dehydroxylated at temperatures of around 400 to 650 °C [21]. Thereby, the hydroxyl groups between the silicate layers are released in a gaseous form as water (eq. (7)). Subsequently, delamination (i.e., deconstruction of the kaolinite structure) and structure modification occur. Al changes from a 6- to 4-fold coordination and Si remains in 4-fold coordination in the tetrahedral sheet. These reactions and modifications are endothermic and result in the highly reactive meta-kaolinite. At higher temperatures of 900 to 1000 °C, exothermic recrystallization may occur [22].

$$Al_2Si_2O_5(OH)_4 \rightarrow Al_2O_3{\cdot}2SiO_2 + 2H_2O \quad (7)$$

Meta-kaolinite, in the amorphous structure of alumina (Al_2O_3) and silica (SiO_2) then reacts with K from the biomass, released as KCl, K_2SO_4, and KOH to form gaseous hydrogen chloride (HCl), sulfur oxide (SO_3), or water (H_2O), as well as K-Al-silicates (i.e., kalsilite ($KAlSiO_4$)) according to eq. (8) till (10). With additional SiO_2 leucite ($KAlSi_2O_6$) and orthoclase ($KAlSi_3O_8$) may also form (not shown)) [23].

$$Al_2O_3{\cdot}2SiO_2 + 2KCl + H_2O \rightarrow 2\,KAlSiO_4 + 2HCl \quad (8)$$

$$Al_2O_3{\cdot}2SiO_2 + K_2SO_4 \rightarrow 2\,KAlSiO_4 + SO_3 \quad (9)$$

$$Al_2O_3{\cdot}2SiO_2 + 2KOH \rightarrow 2\,KAlSiO_4 + H_2O \quad (10)$$

To determine the equilibrium composition of K and additive mixtures at different ratios and temperatures, and to provide indications on ash-related issues in the furnace, thermodynamic calculations can be considered (e.g., in [24] and [25]).

2.2. Aluminum hydroxide ($Al(OH)_3$)

At temperatures of ca. 1000 °C, aluminum hydroxide undergoes an endothermic calcination reaction; i.e., a transformation into aluminum oxide (Al_2O_3) and various crystal modifications as per eq. (11) takes place accompanied by the elimination of water [26]. With silicon dioxide (SiO_2) contained within the solid biofuel, meta-kaolinite may also be formed from aluminum oxide according to eq. (12) to subsequently react with the K to form temperature-stable compounds following eqs. (8) and (9). At approx. 900 °C and in the absence of Si, Al_2O_3 can also bind KCl according to eq. (13) as K-Al-oxide ($KAlO_2$) in the form of a high-temperature stable compound in the ash. However, this reaction is significantly less effective in terms of reducing K emissions than the reaction mechanism via kaolinite [27].

$$2Al(OH)_3 \rightarrow Al_2O_3 + 3H_2O \quad (11)$$

$$Al_2O_3 + 2SiO_2 \rightarrow Al_2O_3{\cdot}2SiO_2 \quad (12)$$

$$Al_2O_3 + 2KCl + H_2O \rightarrow 2KAlO_2 + 2HCl \quad (13)$$

2.3. Muscovite ($KAl_2Si_3AlO_{10}(OH)_2$)

The incorporation of K in K-Al-silicates (i.e., kalsilite, leucite, and/or orthoclase) may occur through the intermediate phase muscovite [28]. Muscovite belongs to the mica mineral group and undergoes gradual endothermic dehydroxylation in a wide temperature range of 800 to 1000 °C [29].

2.4. Titanium dioxide (TiO_2)

TiO_2 and the mineral ilmenite ($FeTiO_3$) can react with ash and TPM-forming K (compounds) to form K-Ti-oxides and K-titanates (e.g., KTi_8O_{16}) [30]. Ilmenite is commonly used as an oxygen carrier in fluidized bed systems, enhancing combustion efficiency (e.g., [31–33]).

3. Material and methods

The combustion trials were conducted at the test stand of the Institute of Environmental Technology and Energy Economics (IUE) at the Technical University of Hamburg (TUHH). The pellet stove with a tilting grate is commercially available (Polly 2.0, Austroflamm) and has a nominal thermal output of 7.8 kW. In previous experiments, the additive concentration of 0.3 $wt\%_{a.r.}$ (a.r. as received) was determined as most effective in CO and TPM reduction with kaolin within the used experimental setup and fuel (refer to supplementary data). Based on this, an additive concentration of 0.3 $wt\%_{a.r}$ was employed for all additives across the experiments here, to minimize the variations in combustion conditions due to varying ash contents of the fuel (i.e., ash from pellets and additives).

For the preparation of the samples, 5 kg wood pellets were mixed with 15 g additive in a conventional concrete mixer for 10 min. Both before and after the mixing process, the fuel was manually sieved with a mesh size of 4 mm to separate the fines. After initial ignition, the stove was heated for approx. one hour until steady-state operation temperature at the nominal load. Temperature and pressure were measured continuously to ensure stable combustion conditions, the flue gas speed was discontinuously measured with a Prandtl probe. For a more detailed description of the measurement section and procedure refer to [34–36]. The TPM emissions during combustion were gravimetrically and discontinuously measured and the chemical composition was subsequently analyzed (section 3.3). For each combustion test, a minimum of 6 serial dust measurements were carried out over a period of approx. 1–2 h. The remaining ash after each combustion trial was collected and analyzed in terms of chemical composition and crystalline phases (section 3.4). All chemical analyses of the TPM and ash samples were performed in triplicates. The flue gas was continuously measured (Wöhler A 550) in terms of composition (i.e., CO, O_2, H_2, NO_x) (section 3.5). As becomes clear with the supplementary data, the mean CO and TPM emissions from the reference combustion experiments (i.e., without additive) demonstrated a high replicability, indicating a high overall reliability.

3.1. Additives

The effects of (K-)Al-(Si-)based additives on mitigating TPM and reducing CO emissions have been investigated based on a variety of additives including kaolin (i.e., kaolinite with impurities), kaolinite, meta-kaolin (i.e., the dehydrated, amorphous structure of kaolinite), aluminum hydroxide, selected as an exclusively Al-based additive, and the K-Al-Si-based (intermediate) products of K incorporation – muscovite (pure and with TiO_2 coating) and kalsilite. Kaolin is obtained by mining naturally occurring mineral deposits, with large deposits reported in the USA, China, and Germany among others [37]. Kaolin possesses low toxicity [38] and is used as paper coating and filler in paints, plastics, and pharmaceuticals [37]. Pure aluminum hydroxide is generally produced as “aluminum hydrate” and may be used in vaccines as adjuvant and for other medical applications [39]. Muscovite/mica is used in cosmetics and food, and large deposits have been reported in Brazil, India, and Madagascar [40]. Muscovite with TiO_2 coating may be used as a cosmetic product [41]. The particle size distributions of the additives were determined in accordance with DIN EN ISO 17827-2 [40].

- Kaolin was supplied by Gebrüder Dorfner GmbH & Co. Kaolin- und Kristallquarzsandwerke KG.
- Kaolinite was purchased from Sigma Aldrich.
- Meta-kaolinite was produced by thermal activation of kaolinite (heating at 650 °C for 2 h).
- Aluminum hydroxide has been delivered by Andrea Wolbring GmbH & Co. KG as “Alumina hydrate”.
- Pure muscovite was obtained as “Mica Fine” from Olionature.
- Muscovite coated with TiO_2 was acquired as “Soft Silver” from Olionature. The composition of the latter varies between 56 and 60 wt% muscovite and 40 to 44 wt% TiO_2 along with small amounts of unspecified impurities from trace elements.
- The additive kalsilite was synthesized from potassium hydroxide (KOH) and kaolinite (molar ratio 2:1). The two reactants were homogeneously mixed with a small amount of water as a solvent and then heated at a maximum of 550 °C for 3 h. After the treatment, the product was ground and then tested for the crystalline compound kalsilite using X-ray diffraction.

The combustion samples and their denotation are shown in Table 1.

3.2. Wood pellets

The wood pellets used are pressed from sawdust from hard- and softwood and certified as quality class A1 pellets in accordance with DIN EN ISO 17225-2 [42]. Table 2 shows the fuel properties and chemical composition of the pellets.

3.3. Total particulate matter (TPM) emissions

The determination of TPM emissions follows a manual, discontinuous, gravimetric methodology in accordance with DIN EN 13284–1 [46] and VDI 2066–1 [47]. This includes sampling a partial volume flow of the flue gas under isokinetic conditions at a representative point within the measuring section, as outlined in DIN EN 15259 [48]. Each sampling duration was 5 min and conducted back-to-back with an outstack filter unit (Paul Gothe). Prior sampling the filters were baked out in a laboratory drying oven (Heraeus LUT 6050) at 160 °C for 1 h and subsequently cooled for a minimum of 8 h in a desiccator. Following the 5 min sampling time, the loaded filters were subjected again to heating, cooling, and re-weighing. In each combustion trial, eight flat filters were sampled. TPM emissions are reported for dry flue gas in mg/Nm^3 with a reference oxygen concentration of 13 vol.-% in the flue gas. In the used furnace, a cleaning cycle is carried out roughly every 50 min during the firing operation by reducing the fuel supply and simultaneously increasing the primary air supply. Sampling of TPM emissions was avoided at this time.

The derived filters were then analyzed in terms of chemical composition by atomic absorption spectrometry (AAS, Analytik Jena contrAA 700) and ion chromatography (IC, Dionex Sodtron ICS-90) (three flat filters each). The sample preparation for the AAS was conducted in accordance with DIN 22022–1 [49] and DIN EN ISO 16967 [50] with aqua regia in a microwave digestion system (Anton Paar Multiwave GO Plus). The IC sample preparation was conducted with deionized water and the water-soluble dissolved anions (e.g., sulfate and chloride) were measured, according to DIN EN ISO 16994 [51] and DIN EN ISO 10304-1 [52].

Table 1
Denotation of the (additivated) wood pellet samples used in the combustion trials.

Sample name	Additive	Formula of Additive
Ref	No additvie	–
Ka	Kaolin	$Al_2Si_2O_5(OH)_4$ + 3.4% impurities
Kao	Kaolinite	$Al_2Si_2O_5(OH)_4$
M-Kao	Meta-kaolinite	$Al_2O_3 \bullet 2SiO_2$
Al-Hyd	Aluminum hydroxide	$Al(OH)_3$
Musc	Muscovite	$KAl_2Si_3AlO_{10}(OH)_2$
Musc + TitOx	Muscovite and titanium dioxide	$KAl_2Si_3AlO_{10}(OH)_2 + TiO_2$
Kal	Kalsilite	$KAlSiO_4$

Table 2
Fuel properties and chemical composition of the used wood pellets (a.r. as received, d.b. dry basis, * calculated by mass difference) [43–45].

Parameter	Unit	Wood Pellets	Method for Analysis
Moisture content	$wt\%_{a.r}$	6.78	ISO 18134-2
Ash content	$wt\%_{d.b.}$	0.59	ISO 18122
HHV	$MJ/kg_{d.b}$	19.27	ISO 18125
Carbon (C)	$wt\%_{d.b.}$	51	ISO 16948/ ISO 16994
Hydrogen (H)	$wt\%_{d.b.}$	6	ISO 16948/ ISO 16994
Oxygen (O)*	$wt\%_{d.b.}$	42	
Nitrogen (N)	$wt\%_{d.b.}$	0.16	ISO 16948/ ISO 16994
Sulfur (S)	$wt\%_{d.b.}$	< 0.2	ISO 16948/ ISO 16994
Calcium (Ca)	$mg/kg_{d.b.}$	865	ISO 16967/ ISO 16994
Potassium (K)	$mg/kg_{d.b.}$	468	ISO 16967/ ISO 16994
Sodium (Na)	$mg/kg_{d.b.}$	< 313	ISO 16967/ ISO 16994
Magnesium (Mg)	$mg/kg_{d.b.}$	159	ISO 16967/ ISO 16994
Phosphorus (P)	$mg/kg_{d.b.}$	142	ISO 16967/ ISO 16994
Manganese (Mn)	$mg/kg_{d.b.}$	89	ISO 16967/ ISO 16994
Silicon (Si)	$mg/kg_{d.b.}$	74	ISO 16967/ ISO 16994
Iron (Fe)	$mg/kg_{d.b.}$	65	ISO 16967/ ISO 16994
Aluminum (Al)	$mg/kg_{d.b.}$	20	ISO 16967/ ISO 16994
Zinc (Zn)	$mg/kg_{d.b.}$	12	ISO 16968
Lead (Pb)	$mg/kg_{d.b.}$	< 0.62	ISO 16968

3.4. Ashes

After each combustion experiment ash samples were taken from the ashtray, homogenized, and analyzed in terms of chemical composition via AAS and IC (compare to section 3.3). In addition to this, the crystalline phases of the ashes were analyzed by X-ray diffraction (XRD, Siemens D500); the existence of the respective crystalline phases was determined using a database (Brucker Diffrac Plus).

3.5. Carbon monoxide (CO) emissions

Every 10 s the CO, as well as CO_2, O_2, H_2, and NO_x emissions were logged using a flue gas analyzer (Wöhler A 550) in the measurement section. The CO emissions are given for dry flue gas in mg/Nm^3 with an oxygen reference concentration of 13 vol.-%.

4. Results and discussion

4.1. Additives

Table 3 shows the composition of the additives, the molar ratios for Si/K and Al/K within the fuel-additive blend, and the median grain sizes $x_{50\%}$. The cumulative particle distributions Q_3 are given in the supplementary data.

Kaolin and kaolinite show with $x_{50\%} = 37$ and $x_{50\%} = 36$, respectively the lowest median grain size $x_{50\%}$ of all used additives. Meta-kaolinite and kalsilite show the highest $x_{50\%}$, most likely due to agglomeration from thermal activation and synthesis. The median grain size may influence the reactive outer surface of the additive. Higher median grain sizes indicate the presence of agglomerates and potentially an uneven/irregular distribution in the pellet surface. The highest Si/K and Al/K ratios are shown for meta-kaolinite with 24.4 and 24.3, respectively, followed by kaolinite. The lowest and highest ratios of Si/K and Al/K, respectively, are displayed for aluminum hydroxide. Here, Si and K are provided only from the fuel, and high amounts of Al are introduced. These molar ratios can be used as indicators for K-release from the fuel: high ratios of Si/K [53] and Al/K [54] indicate low K-release. In Fig. 1 the respective patterns from X-ray diffraction (XRD) (Siemens D5000) of the additive samples are shown. Except for meta-kaolinite and kalsilite, all additives show high crystallinity and a conclusive classification of the crystalline phases. In the case of kalsilite, leucite and orthoclase could also be detected.

4.2. Total Particulate Matter (TPM) emissions

In Fig. 2 the TPM emissions released during wood pellet combustion without and with additives in a small-scale pellet furnace are shown as boxplots. The average of the TPM emissions during the combustion of unadditivated wood pellets in this test series was 30 mg/Nm^3 (corresponding to the valid limit value of 30 mg/Nm^3 defined in the 1. BImSchV [2] for pellet stoves without water pocket) and was significantly reduced by additivation with Al-Si-based minerals – except for kalsilite.

- The additives kaolin, its pure form kaolinite, as well as muscovite, showed the greatest reduction effect of TPM emissions with 15 mg/Nm^3 (−50%), 18 mg/Nm^3 (−40%) and 19 mg/Nm^3 (−37%), respectively. At the same time, the scatter of the individual measured values decreased significantly in most cases compared to the non additivated reference case.
- The TPM-mitigation effect of meta-kaolinite was 24 mg/Nm^3 (−20%) and thus lower than in its initial, non-activated form kaolinite.
- The average TPM emissions for aluminum hydroxide were around 24 mg/Nm^3 (−20%), whereby a comparatively large scattering of the individual measured values was observed, particularly for the latter.
- Compared to pure muscovite (19 mg/Nm^3), the use of muscovite coated with titanium dioxide exhibited a slight increase in TPM emissions to 22 mg/Nm^3 with a simultaneous significant increase in the scatter of the measured values.
- The addition of kalsilite as an additive to the combustion of the wood pellets did not show any reduction in TPM emissions and was with 31 mg/Nm^3 (+3%) even slightly above the level of the reference case.

Table 3
Composition of selected Al-Si-based, Al-based, and K-Al-Si-based materials for wood pellet additivation in a pellet stove, the resulting Si/K and Al/K molar ratios within the fuel-additive blend and the median grain size $x_{50\%}$ of the additives ($^+$ according to the supplier, * 100% purity is assumed, ** within fuel-additive blend).

		Unit	Ka^+	Kao	M-Kao	Al-Hyd	Musc*	Musc + TitOx*	Kal
Composition	SiO_2	$wt\%_{a.r.}$	50.2	46.5	54.1		45.3	37.7	38.0
	Al_2O_3	$wt\%_{a.r.}$	34.4	39.5	45.9	65.4	38.4	32.0	32.2
	H_2O	$wt\%_{a.r.}$	12	14.0		34.6	4.5	3.8	
	CaO	$wt\%_{a.r.}$	< 0.1						
	TiO_2	$wt\%_{a.r.}$	0.4					16.7	
	Fe_2O_3	$wt\%_{a.r.}$	0.5						
	K_2O	$wt\%_{a.r.}$	2.1				11.8	9.8	29.8
	Na_2O	$wt\%_{a.r.}$	0.2						
	MgO	$wt\%_{a.r.}$	< 0.1						
	P_2O_5	$wt\%_{a.r.}$	0.2						
Ratios	Si/K**		10.3	21.1	24.4	0.2	2.2	2.2	0.8
	Al/K**		8.3	20.9	24.3	34.6	2.2	2.2	0.8
Size	$x_{50\%}$	µm	37	36	356	160	105	119	271

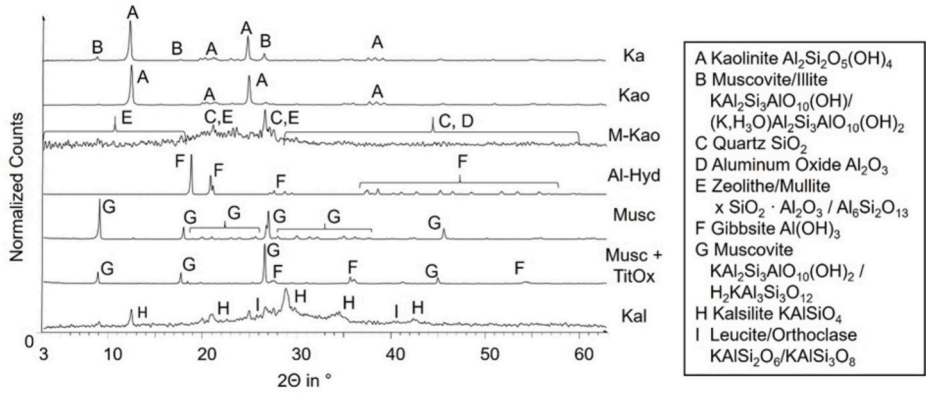

Fig. 1. X-ray diffractogram of additives and detected crystalline phases.

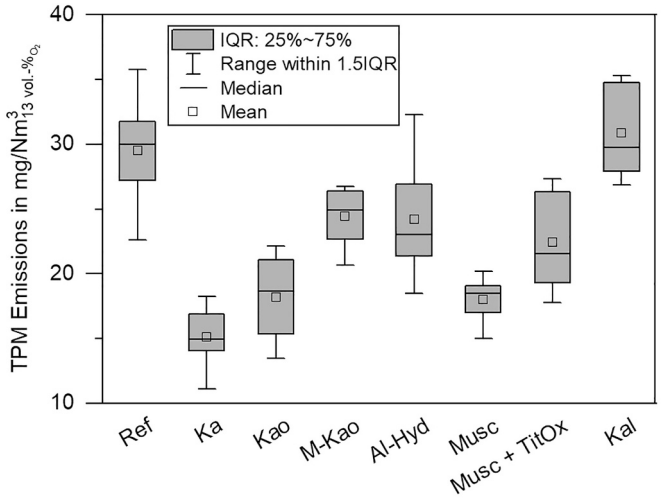

Fig. 2. Total particulate matter (TPM) emissions for wood pellet combustion in a 7.8 kW pellet furnace without (Ref) and with 0.3 wt% additives (IQR: interquartile range, Range within 1.5IQR: minimum value without outliers < Q1–1.5 x IQR, maximum value without outliers > Q3 + 1.5 x IQR).

These results can be discussed as follows.

- The 50% reduction in TPM emissions by kaolin surpasses the reduction effects of its pure form kaolinite. This has also been reported in other investigations (e.g., [34,55]). The exact reasons are not clear so far; some authors suggested the small particle sizes of kaolinite lead to the entrainment of the additive particles with the flue gas [56].
- Meta-kaolinite showed a lower reduction in TPM emissions than the other additives (except for kalsilite), including its "preform" kaolinite. Solely considering the chemical composition, it was anticipated that meta-kaolin would exhibit superior K incorporation effects: Si/K ratio and Al/K ratios were higher than for kaolin and kaolinite, and no endothermic dehydration and structure change, as depicted in eq. (7), was necessary before reactions with the K-compounds could occur. When considering the mean particle size (Table 3), the physical properties of the additive might become relevant: meta-kaolinite shows with 356 μm the highest mean particle size, resulting not only in a potential irregular distribution on the fuel particle surface but also in a lower surface to mass ratio of the additive, reducing the reactive outer surface.
- The diminished TPM reduction observed with aluminum hydroxide can be attributed to the absence of Si when solely Al is introduced through the additive. This implies that K incorporation via meta-kaolinite is reliant on Si present in the biomass. However, the theoretically required molar ratio (SiO_2:Al_2O_3 = 2:1) for the formation of meta-kaolinite (eq. (12)) cannot be achieved due to the insufficient Si concentration in the wood pellets (Table 2). Alternatively, KCl can be incorporated without Si involvement (eq. (13)), forming K-Al-oxide, but this is considered less efficient compared to reactions with kaolin [27].
- For muscovite, despite the low availability of compounds for incorporating the same amount of K from the biomass, reflected in the Si/K and Al/K ratios in Table 3, a substantial reduction in TPM emissions by 37% was observed at the investigated additive concentration of 0.3 wt%. However, muscovite coated with TiO_2 showed a slightly lower reduction in TPM emissions of 27%. The presence of approx. 42 wt% TiO_2 in the additive significantly reduced the amount of the presumably reactive substance (e.g., aluminum and silicon). Although K incorporation and thus a potential TPM mitigation has been reported in the case of TiO_2 addition to solid biofuels [57], the specific contribution of TiO_2 itself does not seem to compensate for the dilution effects of muscovite.
- The slight increase in TPM emissions with kalsilite (in combination with leucite ($KAlSi_2O_6$) and orthoclase ($KAlSi_3O_8$)) by 3% compared to the reference case, goes along with the expectations and the depicted Si/K and Al/K ratios: as a stable reaction product (refer to eqs. (8) till (10)) of K incorporation, kalsilite cannot contribute sufficiently to the reduction of corresponding K from the biomass. However, due to its high melting point and inert nature, the addition of kalsilite leads to an increase in ash content, potentially disrupting the primary air supply and increasing emissions of organic particles.

In Fig. 3 the average chemical compositions of the sampled TPM emissions are shown, and Table 4 denotes the absolute emissions in the flue gas. Sulfate (SO_4^{2-}) and K had the highest share of the sampled TPM for the unadditivated reference case with 347 mg/g_{TPM} and 278 mg/g_{TPM}, respectively. Other significant contents were chloride (Cl^-) (66 mg/g_{TPM}), Ca (37 mg/g_{TPM}), and Na (28 mg/g_{TPM}). Mg and Al had negligible shares within the TPM emissions.

- In the additivation of the wood pellets with kaolin, a notable SO_4^{2-} reduction to 217 mg/g_{TPM} along with a small reduction of K to 258 mg/g_{TPM} becomes pertinent. The share of Ca, Na, and Cl^- in the TPM emissions rose, as well as the share of unidentified components.
- Similar results are shown for kaolinite, although the share of unidentified components (most likely mainly organic particles) rose from 22% (reference case) to 26% (kaolinite).
- Meta-kaolinite demonstrated with 179 mg/g_{TPM}, 14 mg/g_{TPM}, and 148 mg/g_{TPM} the lowest share of K, Na, and SO_4^{2-} in TPM emissions from all additives, though exhibiting the highest share of unidentified compounds (51 wt%).

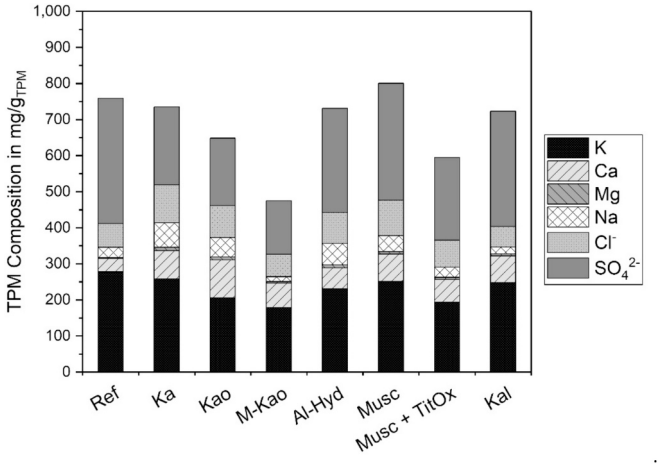

Fig. 3. Chemical composition of TPM emissions from wood pellet combustion in a 7.8 kW pellet furnace without (Ref) and with 0.3 wt% additives.

Table 4
Chemical components in flue gas from wood pellet combustion in a 7.8 kW pellet furnace without (Ref) and with 0.3 wt% additives.

Component in mg/Nm$_3$	Ref	Ka	Kao	M-Kao	Al-Hyd	Musc	Musc + TitOx	Kal
K	8.2 ± 1.3	3.9 ± 0.7	3.7 ± 0.9	4.4 ± 0.5	5.6 ± 1.3	4.6 ± 0.6	4.3 ± 0.8	7.7 ± 1.1
Ca	1.1 ± 0.2	1.2 ± 0.2	1.9 ± 0.6	1.6 ± 0.0	1.4 ± 0.2	1.4 ± 0.3	1.4 ± 0.2	2.3 ± 0.9
Mg	0.1 ± 0.0	0.1 ± 0.1	0.2 ± 0.1	0.1 ± 0.0	0.2 ± 0.2	0.1 ± 0.1	0.1 ± 0.0	0.2 ± 0.1
Na	0.8 ± 0.5	1.0 ± 0.9	1.0 ± 1.1	0.3 ± 0.0	1.4 ± 0.8	0.8 ± 0.6	0.6 ± 0.4	0.6 ± 0.1
Cl$^-$	2.0 ± 0.1	1.6 ± 0.2	1.6 ± 0.3	1.5 ± 0.2	2.1 ± 0.2	1.8 ± 0.1	1.7 ± 0.2	1.8 ± 0.2
SO_4^{2-}	10.2 ± 1.4	3.3 ± 0.5	3.4 ± 0.1	3.6 ± 0.4	7.0 ± 1.5	6.0 ± 0.8	5.1 ± 1.0	9.9 ± 0.8
Other	7.1	4.0	6.4	12.8	6.7	5.0	9.1	6.2

- The TPM emissions for the additivation of the fuel with the additive aluminum hydroxide showed a small decrease in the SO_4^{2-} and K concentrations to 288 mg/g$_{TPM}$ and 232 mg/g$_{TPM}$, respectively, as well as slightly higher proportions of Cl$^-$, Ca, and Na compared to the reference case; the proportion of unidentifiable components was around 25 wt%.
- With a concentration of 325 mg/g$_{TPM}$ for SO_4^{2-} and a K concentration of 250 mg/g$_{TPM}$, the TPM emissions for the additivation of the fuel with muscovite had a similar composition to the reference case. The contents of Na, Cl$^-$, and especially Ca were higher in comparison. The proportion of unidentified components for the additive with pure muscovite was around 17 wt%, while the addition of TiO_2-coated muscovite increased this proportion to around 39 wt%; the composition of the detected inorganic components remained almost the same.
- When kalsilite was used as an additive, the TPM composition seemed to be similar to that of the unadditivated reference case, although, except for Ca, slightly lower concentrations were measured for all main components of the TPM compared to the combustion of pure wood pellets. Conversely, the proportion of unidentifiable TPM components increased to around 25 wt%

SO_4^{2-} and K constituted the primary components of all TPM emissions, resulting from inorganic TPM forming components such as potassium sulfate (K_2SO_4), followed by lower concentrations of Cl$^-$ (e.g., from KCl), Ca, and Na.

- The significant reduction in TPM emissions observed with kaolin addition can be primarily attributed to the incorporation of K from K_2SO_4 in K-Al-silicates (eq. (9)). The thermodynamically favored reactions between K_2SO_4 and meta-kaolinite (Gibb's Energy ΔG to $KAlSiO_4$: $\Delta G = -357$ kJ, to $KAlSi_2O_6$: $\Delta G = -439$ kJ compared to $\Delta G = -318$ kJ and $\Delta G = -399$ kJ, respectively for the reaction of KCl and meta-kaolin [58], eq. (8)), may be one explanation for this higher relative reduction compared to KCl. Despite kaolin addition, the release of Ca, Cl$^-$, and Na into the gas phase during combustion seems to have remained almost unaltered, leading to a relative enrichment of these substances in the TPM emissions, even with approximately constant absolute emissions (Table 4).
- Meta-kaolinite has the lowest relative share of K, Na, and SO_4^{2-} in the measured TPM emissions, yet the absolute emissions of K and SO_4^{2-} in the flue gas (i.e., in mg/Nm^3) are higher than with kaolin and kaolinite. This indicates less effective K incorporation, though being the "active" form of kaolinite.
- The reduction in TPM emissions due to aluminum hydroxide addition can be mainly attributed to the suppression of SO_4^{2-} and K release. However, compared to kaolin addition, the reduction in absolute emissions for K is about 20%, and for SO_4^{2-} approx. 36% less than for kaolin. This limitation is attributed to the restricted availability of intrinsic Si from the biomass needed for the formation of meta-kaolinite necessary for subsequent reactions with K_2SO_4.
- For muscovite as an additive, the significant reduction in TPM emissions is primarily attributed to the suppression of K release, albeit slightly weaker than observed for kaolinite. The decrease in the SO_4^{2-} fraction in the TPM is less pronounced.
- The TPM emissions from combustion experiments with wood pellets and muscovite with TiO_2 as an additive showed a nearly identical relative composition of the identified elements compared to that of pure muscovite. This mixture results in a minor further reduction in absolute emissions of K, SO_4^{2-}, and Cl$^-$. This observation suggests that TiO_2 also contributes to reducing TPM emissions during wood pellet combustion, which has been observed elsewhere (e.g., [59,60]).
- In contrast, the slight increase in TPM emissions with kalsilite addition compared to the reference case can be explained by an enhanced release of incompletely burned organic particles. Kalsilite, as an inert and temperature-stable reaction product of K incorporation, leads to an increased ash content in the combustion chamber, potentially disrupting the primary air supply and resulting in poorer solid combustion. Minor reductions in absolute emissions of SO_4^{2-}, Cl$^-$, and K may be attributed to the presence of unreacted kaolinite from the synthesis process available for K incorporation.

4.3. Ashes - chemical composition and crystalline phases

The composition of the ash from the pellet combustion series is shown in Fig. 4. For all cases, significant contents of K, Ca, Mg, and Al have been identified, while Na, Cl$^-$, and SO_4^{2-} showed low, and in the case of Na almost negligible amounts. Most parts of the ashes (57% and 66% for the reference case and kaolin, respectively) were not identified but assumed to be incompletely burned fuel particles, as well as silicates and oxides, which align with the detected crystalline phases (Table 5). The Ca concentration in the ash decreased from 225 mg/g$_{ash}$ in the reference case to 157 mg/g$_{ash}$ and 156 mg/g$_{ash}$ for the addition of kaolin and kaolinite, respectively. The average Ca concentration in the ash for the other additives was 185 mg/g$_{ash}$. After Ca, the concentration of K in the ash was highest with about 125 mg/g$_{ash}$ for unadditivated wood pellets. As a result of the addition of the various additives, the K content

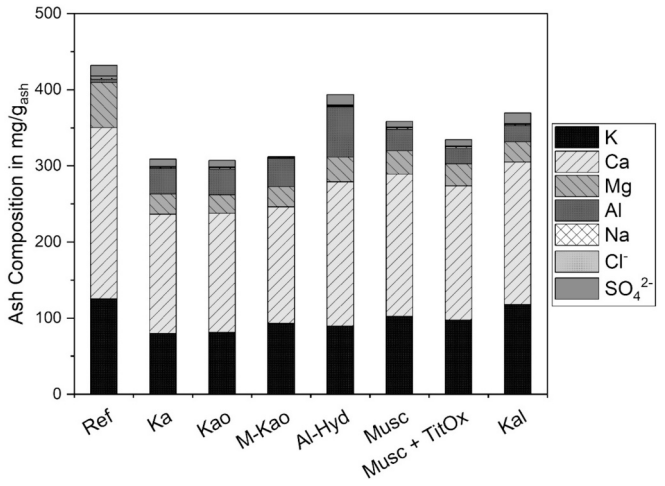

Fig. 4. Chemical composition of ash from wood pellet combustion in a 7.8 kW pellet furnace without (Ref) and with 0.3 wt% additives.

Table 5
Detected crystalline phases of the combustion ash of wood pellets without (Ref) and with 0.3 wt% additives from XRD analysis.

	Ref	Ka	Kao	M-Kao	Al-Hyd	Musc	Musc + TitOx	Kal
MgO	x	x	x	x	x	x	x	x
CaO	x	x	x	x	x		x	x
SiO_2	x	x	x		x			
$CaSO_4$	x			x				x
$KAlSiO_4$		x	x	x	x	x	x	x
$KAlSi_2O_6$						x		
$KAlSi_3O_8$		x				x	x	
$Ca_3Al_2Si_3O_{12}$		x	x			x	x	x
$CaAl_2Si_2O_8$					x			

decreases on average to 95 mg/g$_{ash}$, while comparatively higher concentrations of 103 mg/g$_{ash}$ and 118 mg/g$_{ash}$ could be measured for (K-containing) muscovite and kalsilite. For Mg, a halving of the content in the ash from 59 mg/g$_{ash}$ in the reference case to an average of 28 mg/g$_{ash}$ for the use of the various additives was observed, possibly due to dilution effects attributed to the higher amount of ash. The content of Al in the ash, on the other hand, showed a significant increase as a result of the additives. While the concentration for the combustion of pure wood pellets was around 5 mg/g$_{ash}$, concentrations of 29 mg/g$_{ash}$ could be measured for the addition of muscovite, 34 mg/g$_{ash}$ for the kaolin and kaolinite additives, 37 mg/g$_{ash}$ for meta-kaolinite and 66 mg/g$_{ash}$ for aluminum hydroxide. The Al concentration for the additives kalsilite and muscovite with TiO_2 averaged at 21 mg/g$_{ash}$ each.

The XRD analysis identified crystalline compounds in the ash samples (Table 5). The results reveal the presence of magnesium oxide (MgO) and calcium oxide (CaO) in almost all ash samples. Silicon dioxide (SiO_2) was also detectable in the ash for some additivated samples, similar to the reference case. In addition, kalsilite ($KAlSiO_4$), leucite ($KAlSi_2O_6$), and orthoclase ($KAlSi_3O_8$) were detected in the ash for all additives used, as well as for muscovite and kaolin. Furthermore, calcium sulfate ($CaSO_4$) and calcium aluminum silicates ($CaAl_2Si_2O_8$, $Ca_3Al_2Si_3O_{12}$) were found in the ash for various fuel samples.

The analysis of ash samples from additivated fuels discloses a substantial increase in Al concentrations, corresponding with the introduced Al content from the additives. This correlation is especially evident in the case of aluminum hydroxide, disclosing a notably high Al concentration. Similar considerations apply to the K-content within the ash, which are highest for muscovite and kalsilite, introducing the highest share of K from the additive into the fuel-additive blend. However, the highest K-content within the ash is measured in the reference case without additive. This is plausible when considering the lower ash content for the reference case compared to the additivated fuels: by additivation, inorganic material is introduced with the wood into the combustion chamber, raising the ash content of the fuel mixture from 0.59 wt% (ash from wood pellets alone) to 0.89 wt% (pellet ash + additive). This results in a dilution of some elements (e.g., K, Ca, and Mg) in the ash by >50%. The actual increase in bottom ash is even higher when accounting for the incorporation of elements (e.g., K). For instance, in the ash from kaolin additivation compared to the reference case, the K share is reduced by 36%, Ca by 30%, Mg by 55%, and Cl^- by 62%, even though higher incorporation of K within is the case.

XRD analysis substantiates the presence of kalsilite in the ash for all additives, proving the incorporation of K in the form of temperature-stable K-Al-silicates as per eqs. (8) till (10) (excluding the additive kalsilite, since no additional incorporation can be determined with certainty via XRD). For the muscovite-based additives, leucite ($KAlSi_2O_6$) and orthoclase ($KAlSi_3O_8$) are notable reaction products formed. The crystalline composition of muscovite (K_2O:Al_2O_3:SiO_2 = 1:3:6) favors the formation of these compounds during K incorporation.

4.4. Carbon monoxide (CO) emissions

The CO emissions evolved during the combustion of the wood pellets without additives for the reference case and with respective additive concentrations of 0.3 wt% during the experiments are shown in Fig. 5.

Approximately every 50 min the CO emissions peak due to the regular cleaning mode. Here, the primary air supply is increased to blow out the ash from the combustion bowl resulting in a high excess air ratio and lower temperatures in the combustion chamber. This leads to higher emissions from incomplete combustion. The highest peaks were reached in the reference case with 13,900 and 23,000 mg/Nm^3 for the first and the second peak, respectively. The lowest level of emission and the lowest fluctuation of emissions were measured in the case of additivated pellets with kaolin, aluminum hydroxide, muscovite, and muscovite with TiO_2. Fig. 6 shows the boxplots of the CO emissions, with the emissions released during the cleaning mode excluded from the calculation.

- In the unadditivated reference case, the CO emissions showed an average value were 498 mg/Nm^3.
- By adding kaolin, the CO emissions could be reduced to a mean value of 237 mg/Nm^3 (−52%).
- Pure kaolinite showed slightly higher CO emissions than kaolin at 344 mg/Nm^3 (−31%), its activated form meta-kaolinite showed CO emissions of 603 mg/Nm^3 (+21%) and thus even higher than the reference case.
- The addition of aluminum hydroxide resulted in a slight reduction (with 432 mg/Nm^3, −13%) compared to the reference case.
- Introducing muscovite reduced the CO emissions to a level of 265 mg/Nm^3 (−47%), close to the level of kaolin.
- The addition of muscovite with TiO_2 slightly increased the emissions compared to muscovite, reaching an average of 364 mg/Nm^3 (−27%).
- Kalsilite led to an elevation in CO emissions to an average of 838 mg/Nm^3 (+68%) and a considerable variability in the measured values.

The results can be discussed as follows:

- The 31% reduction in CO emissions by kaolinite, compared to the reduction effects of kaolin (−52%), is consistent with the results observed in other investigations (e.g., [34,55]). This prompts further investigation, including exploration of potential synergistic effects contributing to the enhanced performance of kaolin in mitigating TPM emissions.
- When comparing the effects of respective additives on CO emissions with the effects on TPM emissions, similar mitigation dimensions are

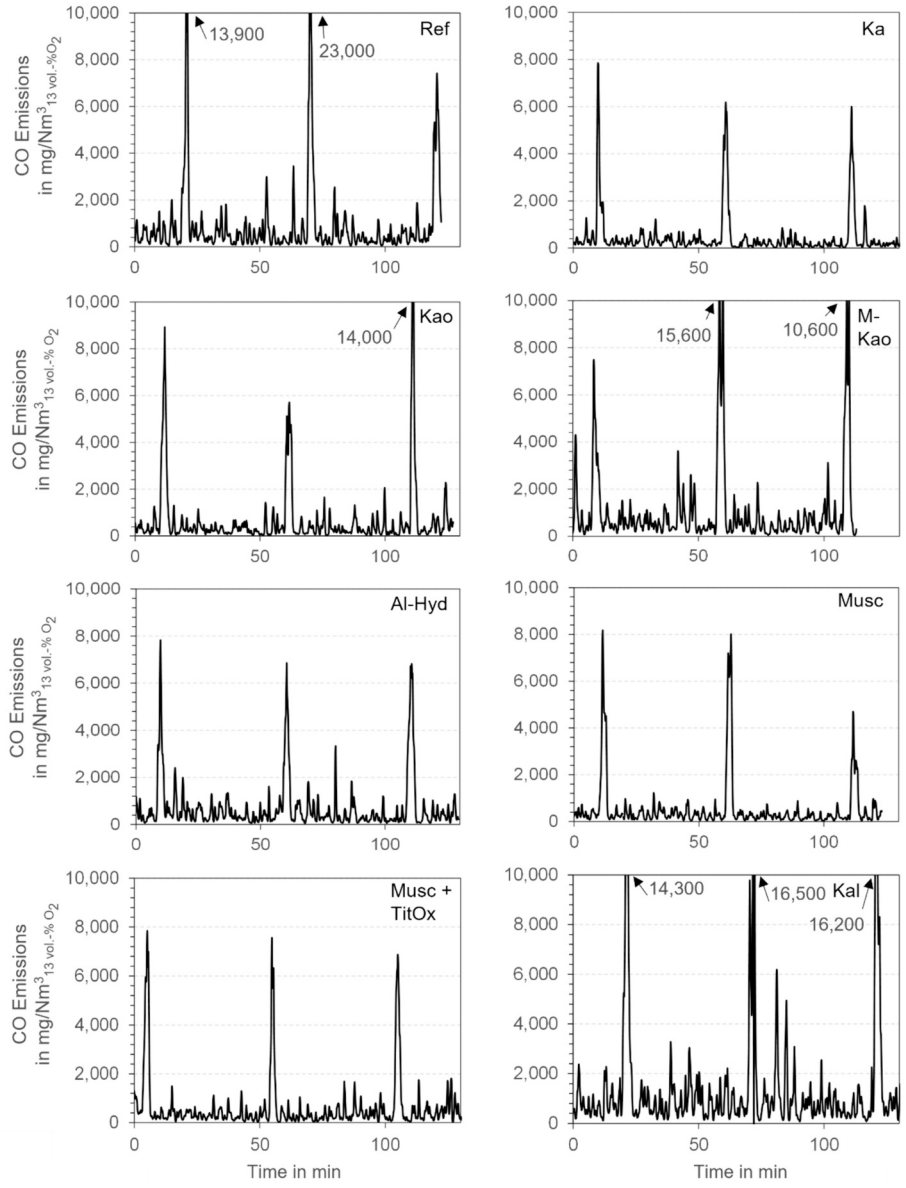

Fig. 5. CO emissions during wood pellet combustion in a 7.8 kW pellet furnace without (Ref) and with 0.3 wt% additives, respectively.

observed for kaolin, kaolinite, muscovite (+ TiO_2), and aluminum hydroxide. Since the reduction of TPM emissions is mainly due to K incorporation, the simultaneous mitigation of CO emission is plausible, as outlined in section 1. KCl and KOH in the gas phase lead to reactions with radicals (eq. (2) till (6)), resulting in a decrease of the radical pool, inhibiting CO oxidation. Thus, by K incorporation this interference with the radical pool is avoided, overall leading to a higher radical availability for CO oxidation.

- Meta-kaolinite resulted in a decrease in TPM emissions due to K incorporation, while CO emissions increased, suggesting incomplete combustion. This is consistent with the high share of unidentifiable components within the TPM emissions, potentially attributable to organic emissions. Albeit K incorporation of meta-kaolinite is not as effective as for kaolinite, other reasons for incomplete combustion may be considered here: the conversion of kaolinite to meta-kaolinite, during which water is released at temperatures of 450 to 600 °C was outsourced here. The release of water at these temperatures, even in small amounts, could serve as a local catalyst/radical supplier (e.g., $^{\bullet}OH$ and $H^{\bullet}$ radicals) for gasification and oxidation in the firebed.
- Aluminum hydroxide also exhibits the potential to reduce CO emissions, possibly by incorporating K into the ash (e.g., as in eq. (13)), thereby reducing K release into the gas phase. This mitigates the inhibition of CO oxidation due to interference of K with radicals in the gas phase, which are crucial for CO oxidation. However, the reduction is less pronounced compared to kaolin, attributed to the lower availability of SiO_2.
- Muscovite demonstrated the highest CO (and TPM) mitigation potential after kaolin, despite relatively low Si/K and Al/K ratios and higher median particle size. In line with this, the K content in the flue gas showed less absolute K incorporation than kaolin, kaolinite, and meta-kaolinite, and the share of unidentifiable (including organic) compounds was the lowest among all additives. This suggests better combustion efficiency, which is also reflected in the CO emissions. The dehydroxylation and associated radical supply in the temperature ranges of 800 to 1000 °C could also have an effect, as outlined above for meta-kaolin.
- Combining muscovite with TiO_2 resulted in a slight decrease in CO mitigation compared to pure muscovite due to a quasi-dilution effect. While positive effects of TiO_2 have been reported, they are not

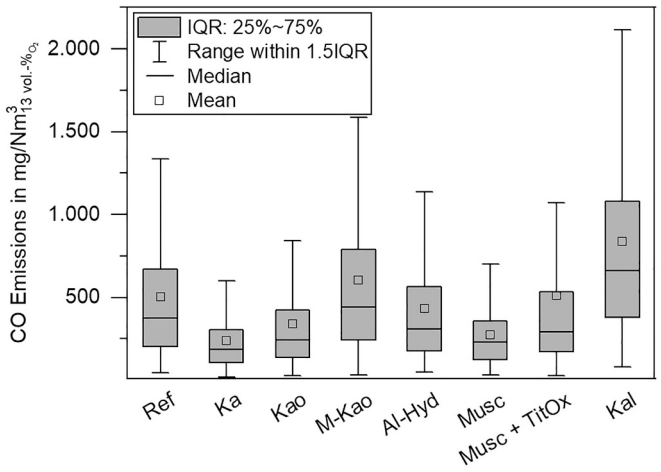

Fig. 6. CO emissions from wood pellet combustion in a 7.8 kW pellet furnace without (Ref) and with 0.3 wt% additives (IQR: interquartile range, Range within 1.5IQR: minimum value without outliers < Q1–1.5 x IQR, maximum value without outliers > Q3 + 1.5 x IQR).

sufficient to counterbalance K incorporation and CO oxidation; additionally potential accessibility limitations to muscovite due to the coating of TiO_2 may be pertinent.

- Kalsilite shows the highest CO emissions, with an increase to the reference case of almost 70%. With the introduction of kalsilite, one final product of K incorporation is introduced (refer to eq. (8)), which makes it evident that for further K incorporation into leucite ($KAlSi_2O_6$) and/or orthoclase ($KAlSi_3O_8$) additional SiO_2 (i.e., from the biomass) would be necessary. According to the XRD results (Table 5) this is not the case. However, the significant rise in CO emissions compared to the reference case without additive could be caused by unreacted KOH left from the synthesis, inhibiting CO oxidation [61]. TPM emissions do not rise in the same order of magnitude: this may be because although KOH is a contributor to (T)PM emissions, the components K_2SO_4 and KCl have been suggested to be the larger contributors to PM formation [62]. The influence of the additional KOH on TPM emissions thus might be limited. The results disprove previous hypotheses suggesting that kalsilite or K-Al-silicates may act as catalysts for CO oxidation and thus CO mitigation in the flue gas. The introduction of primarily inert material increased the ash content and also potentially introduced parts of unreacted KOH and (meta-)kaolinite. KOH may evaporate into the gas phase, leading to a further inhibition of CO oxidation.

5. Conclusion

This paper examines the mitigation potentials for TPM and CO emissions from wood pellet combustion with (K-)Al-(Si-)based additives. The effectiveness of these additives in reducing TPM emissions, compared to the reference case, is as follows: kaolin > muscovite > kaolinite > muscovite + TiO_2 > aluminum hydroxide > meta-kaolinite > kalsilite, with a slight increase in emissions observed for kalsilite. The same order is valid for CO emissions, suggesting K as the main connector between TPM and CO emissions.

- Kaolin exhibits the highest mitigation effects in both TPM and CO emissions, surpassing even kaolinite.
- Muscovite also shows significant TPM reduction, though the reduction of K-originated TPM is relatively low. This is attributed to the smaller K incorporation potential, coupled with high combustion efficiency. The latter could be enhanced by the slow dehydroxylation of muscovite, providing a local radical supply at temperatures of 800 to 1000 °C.
- Muscovite coated with TiO_2 has a reduced effectiveness due to lower SiO_2 and Al_2O_3 availability, which is not compensated by the positive effects of TiO_2.
- Due to the low content of SiO_2 (i.e., only from within the fuel), aluminum hydroxide primarily incorporates K as K-Al-oxides, which is thermodynamically less favored than incorporation in K-Al-silicates.

Meta-kaolinite and kalsilite show higher discrepancies between their effects on TPM and CO emissions.

- Meta-kaolinite unexpectedly shows lower TPM mitigation effects compared to kaolinite, likely due to poorer combustion conditions and insufficient air supply, which are evident in high CO emissions.
- Kalsilite leads to a significant increase in CO emissions, possibly due to unreacted KOH from the synthesis, evaporating into the gas phase and inhibiting CO oxidation. The TPM emissions do not rise accordingly; this may be because the influence of KOH plays a subordinate role in TPM emission formation compared to KCl and K_2SO_4.

CRediT authorship contribution statement

Theresa Siegmund: Writing – original draft, Validation, Investigation, Conceptualization. **Christian Gollmer:** Writing – review & editing, Investigation. **Niklas Horstmann:** Writing – review & editing, Investigation. **Martin Kaltschmitt:** Writing – review & editing, Supervision.

Declaration of generative AI and AI-assisted technologies in the writing process

During the preparation of this work the authors used ChatGPT 3.5, only in order to improve readability and language. After using this tool/service, the authors reviewed and edited the content as needed and take full responsibility for the content of the publication.

Declaration of competing interest

The authors declare that they have no known competing financial interests or personal relationships that could have appeared to influence the work reported in this paper.

Data availability

Data will be made available on request.

Appendix A. Supplementary data

Supplementary data to this article can be found online at https://doi.org/10.1016/j.fuproc.2024.108111.

References

[1] Umweltbundesamt: Erneuerbare Energien in Deutschland. Daten zur Entwicklung im Jahr 2022, 2023.
[2] Bundesamt für Justiz: Erste Verordnung zur Durchführung des Bundes-Immissionsschutzgesetzes (Verordnung über kleine und mittlere Feuerungsanlagen - 1. BImSchV) n.d.
[3] E.D. Vicente, C.A. Alves, An overview of particulate emissions from residential biomass combustion, Atmos. Res. 199 (2018) 159–185, https://doi.org/10.1016/j.atmosres.2017.08.027.
[4] Statista: Preisentwicklung für Holzpellets in Deutschland in den Jahren 2013 bis 2023 (in Euro pro Tonne). https://de.statista.com/statistik/daten/studie/214738/umfrage/preisentwicklung-fuer-holzpellets-in-deutschland/, 2023.
[5] Statista: Preisentwicklung von Kaolin in den Jahren von 2006 bis 2012. https://de.statista.com/statistik/daten/studie/246402/umfrage/preisentwicklung-von-kaolin/, 2012.
[6] Statista: Average price of kaolin in the U.S. from 2010 to 2023. https://www.statista.com/statistics/248194/average-price-of-kaolin/, 2023.

[7] J.L. Míguez, J. Porteiro, F. Behrendt, D. Blanco, D. Patiño, A. Dieguez-Alonso, Review of the use of additives to mitigate operational problems associated with the combustion of biomass with high content in ash-forming species, Renew. Sust. Energ. Rev. 141 (2021), https://doi.org/10.1016/j.rser.2020.110502. S. 110502.
[8] L.S. Bäfver, M. Rönnbäck, B. Leckner, F. Claesson, C. Tullin, Particle emission from combustion of oat grain and its potential reduction by addition of limestone or kaolin, Fuel Process. Technol. 90 (3) (2009) 353–359, https://doi.org/10.1016/j.fuproc.2008.10.006.
[9] M. Bellotto, A. Gualtieri, G. Artioli, S.M. Clark, Kinetic study of the kaolinite-mullite reaction sequence. Part I: Kaolinite dehydroxylation, Phys. Chem. Miner. 22 (1995), https://doi.org/10.1007/BF00202253.
[10] M. Gehrig, M. Wöhler, S. Pelz, J. Steinbrink, H. Thorwarth, Kaolin as additive in wood pellet combustion with several mixtures of spruce and short-rotation-coppice willow and its influence on emissions and ashes, Fuel 235 (2019) 610–616, https://doi.org/10.1016/j.fuel.2018.08.028.
[11] R. Mack, D. Kuptz, C. Schön, H. Hartmann, Combustion behavior and slagging tendencies of kaolin additivated agricultural pellets and of wood-straw pellet blends in a small-scale boiler, Biomass Bioenergy 125 (2019) 50–62, https://doi.org/10.1016/j.biombioe.2019.04.003.
[12] R. Mack, C. Schön, D. Kuptz, H. Hartmann, T. Brunner, I. Obernberger, H.M. Behr, Influence of wood species and additives on emission behavior of wood pellets in a residential pellet stove and a boiler, Biomass Convers. Biorefinery (2023), https://doi.org/10.1007/s13399-023-04204-x.
[13] Z. Zhang, J. Liu, F. Shen, Y. Dong, Insights into the effects of atmosphere and chlorine on potassium release during biomass combustion: temporal measurement and kinetic studies, Energy Fuel 32 (12) (2018) 12523–12531, https://doi.org/10.1021/acs.energyfuels.8b02399.
[14] L.S. Johansson, C. Tullin, B. Leckner, P. Sjövall, Particle emissions from biomass combustion in small combustors, Biomass Bioenergy 25 (4) (2003) 435–446, https://doi.org/10.1016/S0961-9534(03)00036-9.
[15] I. Höfer, T. Huelsmann, M. Kaltschmitt, Influence of Ca- and Al-additives on the pollutant emissions from blends of wood and straw in small-scale combustion, Biomass Bioenergy 150 (2021) 1. S. 106135.
[16] S. Xiong, J. Burvall, H. Örberg, G. Kalen, M. Thyrel, M. Öhman, D. Boström, Slagging characteristics during combustion of corn stovers with and without Kaolin and Calcite, Energy Fuel 22 (5) (2008) 3465–3470, https://doi.org/10.1021/ef700718j.
[17] T. Siegmund, C. Gollmer, M. Scherzinger, M. Kaltschmitt, Submitted Manuscript: CO Emissions during Solid Biofuel Combustion - Formation Mechanisms and Fuel-related Reduction Measures, 2023.
[18] S.R. Turns, An Introduction to Combustion - Concepts and Applications, 3rd ed., McGraw-Hill, Boston, 2011.
[19] A. Chanpirak, H. Wu, P. Glarborg, P. Marshall, An experimental and chemical kinetic modeling study of the role of potassium in the moist oxidation of CO, Fuel 335 (2023), https://doi.org/10.1016/j.fuel.2022.127075. S. 127075.
[20] K.-Q. Tran, K. Iisa, B.-M. Steenari, O. Lindqvist, A kinetic study of gaseous alkali capture by kaolin in the fixed bed reactor equipped with an alkali detector, Fuel 84 (2–3) (2005) 169–175, https://doi.org/10.1016/j.fuel.2004.08.019.
[21] B.-M. Steenari, O. Lindqvist, High-temperature reactions of straw ash and the anti-sintering additives kaolin and dolomite, Biomass Bioenergy 14 (1) (1998) 67–76, https://doi.org/10.1016/S0961-9534(97)00035-4.
[22] Q. Wan, F. Rao, S. Song, Reexamining calcination of kaolinite for the synthesis of metakaolin geopolymers - roles of dehydroxylation and recrystallization, J. Non-Cryst. Solids 460 (2017) 74–80, https://doi.org/10.1016/j.jnoncrysol.2017.01.024.
[23] L. Wang, J.E. Hustad, Ø. Skreiberg, G. Skjevrak, M. Grønli, A critical review on additives to reduce ash related operation problems in biomass combustion applications, Energy Procedia 20 (2012) 20–29, https://doi.org/10.1016/j.egypro.2012.03.004.
[24] T. de Riese, S. Fendt, H. Spliethoff, Utilising thermodynamic equilibrium calculations to model potassium capture by aluminosilicate additives in biomass combustion plants, Fuel 340 (2023), https://doi.org/10.1016/j.fuel.2023.127591. S. 127591.
[25] F. Li, B. Yu, J. Li, Z. Wang, M. Guo, H. Fan, T. Wang, Y. Fang, Exploration of potassium migration behavior in straw ashes under reducing atmosphere and its modification by additives, Renew. Energy 145 (2020) 2286–2295, https://doi.org/10.1016/j.renene.2019.07.141.
[26] L. Reh, Calcination von Aluminiumhydroxid in einer zirkulierenden Wirbelschicht, Chem. Ingen. Tech. 42 (7) (1970) 447–451, https://doi.org/10.1002/cite.330420705.
[27] S. Kyi, B.L. Chadwick, Screening of potential mineral additives for use as fouling preventatives in Victorian brown coal combustion, Fuel 78 (7) (1999) 845–855, https://doi.org/10.1016/S0016-2361(98)00205-1.
[28] L. Wang, G. Skjevrak, J.E. Hustad, Ø. Skreiberg, Investigation of biomass ash sintering characteristics and the effect of additives, Energy Fuel 28 (1) (2014) 208–218, https://doi.org/10.1021/ef401521c.
[29] F. Gridi-Bennadji, B. Beneu, J.P. Laval, P. Blanchart, Structural transformations of Muscovite at high temperature by X-ray and neutron diffraction, Appl. Clay Sci. 38 (3–4) (2008) 259–267, https://doi.org/10.1016/j.clay.2007.03.003.
[30] A. Corcoran, J. Marinkovic, F. Lind, H. Thunman, P. Knutsson, M. Seemann, Ash properties of ilmenite used as bed material for combustion of biomass in a circulating fluidized bed boiler, Energy Fuel 28 (12) (2014) 7672–7679, https://doi.org/10.1021/ef501810u.
[31] T. Schneider, J. Krumrein, D. Müller, J. Karl, Investigation of the oxygen supply and distribution in a bubbling fluidized bed by using natural ilmenite for oxygen carrier aided combustion, Energy Fuel 35 (15) (2021) 12352–12366, https://doi.org/10.1021/acs.energyfuels.1c01178.
[32] L. Duan, L. Li, Oxygen-Carrier-Aided Combustion Technology for Solid-Fuel Conversion in Fluidized Bed, 1st ed., Springer Nature Singapore; Imprint Springer, Singapore, 2023.
[33] Ivana Staničić, Tobias Mattisson, Rainer Backman, Yu Cao, Magnus Rydén: Oxygen Carrier Aided Combustion (OCAC) of Two Waste Fuels - Experimental and Theoretical Study of the Interaction Between Ilmenite and Zinc, Copper and Lead, n.d.
[34] T. Hülsmann, V. Kovač, Feinstaubemissionen bei der Verbrennung von Holz- und Holz/Stroh-Mischpellets - Einfluss einer Brennstoffadditivierung, Schriftenreihe technische Forschungsergebnisse, Verlag Dr. Kovač, 2019.
[35] T. Huelsmann, R. Mack, M. Kaltschmitt, H. Hartmann, Influence of kaolinite on the PM emissions from small-scale combustion, Biomass Convers. Biorefinery 9 (1) (2019) 55–70, https://doi.org/10.1007/s13399-018-0316-8.
[36] C. Gollmer, V. Weigel, M. Kaltschmitt, Emission Mitigation by Aluminum-Silicate-Based Fuel Additivation of Wood Chips with Kaolin and Kaolinite, Energies 16 (2023), https://doi.org/10.3390/en16073095, 7, S. 3095.
[37] National Center for Biotechnology Information, PubChem Compound Summary for CID 56841936, Kaolin. https://pubchem.ncbi.nlm.nih.gov/compound/Kaolin, 2024.
[38] A. Rodriguez-Garraus, M. Alonso-Jauregui, A.-G. Gil, I. Navarro-Blasco, A. López de Cerain, A., Azqueta: genotoxicity and toxicity assessment of a formulation containing silver nanoparticles and Kaolin: an in vivo integrative approach, Nanomaterials (Basel, Switzerl.) 13 (2022), https://doi.org/10.3390/nano13010003.
[39] N. N. Shon, T. Yarbrough, P. Patel: Aluminum Hydroxide, StatPearls, Treasure Island (FL): StatPearls Publishing, https://www.ncbi.nlm.nih.gov/books/NBK546669/, 2023.
[40] National Minerals Information Center, Mica (Natural) - U.S. Geological Survey, Mineral Commodity Summaries. https://www.usgs.gov/centers/national-minerals-information-center/mica-statistics-and-information, 2024.
[41] OLIONATURA®: Mica Fine - C.I. 77019 / Mica. https://www.olionatura.com/shop/kosmetikpigmente/weisspigmente-und-puderstoffe/mica-fine/, 2024.
[42] Deutsches Institut für Normungen e.V.: DIN EN ISO 17225-2 Biogene Festbrennstoffe - Brennstoffspezifikationen und -klassen – Teil 2: Klassifizierung von Holzpellets, n.d.
[43] H. Diedrich, A. Stahl, H. Frerichs, NCHS-Elementaranalyse. M02.001 - Technische Universität Hamburg, Zentrallabor Chemische Analytik, Hamburg, 2022.
[44] H. Cöllen, H. Frerichs, A. Stahl, Elementbestimmung per ICP-MS, Technische Universität Hamburg, Zentrallabor Chemische Analytik, Hamburg, 2022.
[45] C. Fütterer, A. Stahl, Elementbestimmung mit ICP-OES. M02.015, Technische Universität Hamburg, Zentrallabor Chemische Analytik, Hamburg, 2022.
[46] Deutsches Institut für Normungen e.V.: DIN EN 13284–1:Emissionen aus stationären Quellen – Ermittlung der Staubmassenkonzentration bei geringen Staubkonzentrationen, Teil 1: Manuelles gravimetrisches Verfahren, 2018. ICS 13.040.40.
[47] Deutsches Institut für Normungen e.V.: VDI 2066 Blatt 1: Messen von Partikeln Staubmessung in strömenden Gasen Gravimetrische Bestimmung der Staubbeladung, 2019.
[48] Deutsches Institut für Normungen e.V.: DIN EN 15259: Luftbeschaffenheit – Messung von Emissionen aus stationären Quellen – Anforderungen an Messstrecken und Messplätze und an die Messaufgabe, den Messplan und den Messbericht, n.d.
[49] Deutsches Institut für Normungen e.V.: DIN 22022–1: Feste Brennstoffe – Bestimmung der Gehalte an Spurenelementen – Teil 1: Allgemeine Regeln, Probenahme und Probenvorbereitung – Vorbereitung der Analysenprobe für die Bestimmung (Aufschlussverfahren), n.d.
[50] Deutsches Institut für Normungen e.V.: DIN EN ISO 16967: Biogene Festbrennstoffe – Bestimmung von Hauptelementen – Al, Ca, Fe, Mg, P, K, Si, Na und Ti, n.d.
[51] Deutsches Institut für Normungen e.V.: DIN EN ISO 16994: Solid biofuels – Determination of Total Content of Sulfur and Chlorine n.d.
[52] Deutsches Institut für Normungen e.V.: DIN EN ISO 10304-1: Water Quality – Determination of Dissolved Anions by Liquid Chromatography of ions – Part 1: Determination of Bromide, Chloride, Fluoride, Nitrate, Nitrite, Phosphate and Sulfate n.d.
[53] R. Mack, C. Schön, H. Hartmann, T. Brunner, I. Obernberger, TFZ-Bericht 74: Erweiterte Holzpelletcharakterisierung - Einfluss bekannter und neuer Brennstoffparameter auf die Emissionen aus Pelletöfen und -kesseln, 2022.
[54] Q. Liu, W. Zhong, J. Zhou, Z. Yu, Effects of S and Al on K migration and transformation during coal and biomass Co-combustion, ACS Omega 7 (18) (2022) 15880–15891, https://doi.org/10.1021/acsomega.2c00994.
[55] N. Dragutinović, I. Höfer, M. Kaltschmitt, Fuel improvement measures for particulate matter emission reduction during corn cob combustion, Energies 14 (2021) 15, 4548, https://doi.org/10.3390/en14154548.
[56] K.O. Davidsson, B.-M. Steenari, D. Eskilsson, Kaolin Addition during Biomass Combustion in a 35 MW Circulating Fluidized-Bed Boiler, Energy Fuel 21 (4) (2007) 1959–1966, https://doi.org/10.1021/ef070055n.
[57] H. Wiinikka, C. Grönberg, O. Öhrman, D. Boström, Influence of TiO 2 Additive on vaporization of potassium during straw combustion, Energy Fuel 23 (11) (2009) 5367–5374, https://doi.org/10.1021/ef900544z.
[58] I. Höfer, Vollständige Thermochemische Umwandlung Naturbelassener und Additivierter Biogener Festbrennstoffe, DoctoralThesis, Technische Universität Hamburg, 2019.
[59] C. Gollmer, I. Höfer, D. Harms, M. Kaltschmitt, Potential additives for small-scale wood chip combustion – Laboratory-scale estimation of the possible inorganic

particulate matter reduction potential, Fuel 254 (1) (2019), https://doi.org/10.1016/j.fuel.2019.115695. S. 115695.
[60] Y. Xu, X. Liu, Y. Zhang, W. Sun, Y. Hu, M. Xu, A novel Ti-based sorbent for reducing ultrafine particulate matter formation during coal combustion, Fuel 193 (2017) 72–80, https://doi.org/10.1016/j.fuel.2016.12.043.
[61] A. Chanpirak, H. Hashemi, F.J. Frandsen, H. Wu, P. Glarborg, P. Marshall, The chemical coupling between moist CO oxidation and gas-phase potassium sulfation, Fuel 336 (2023), https://doi.org/10.1016/j.fuel.2022.127127. S. 127127.
[62] K.A. Christensen, M. Stenholm, H. Livbjerg, The formation of submicron aerosol particles, HCl and SO2 in straw-fired boilers, J. Aerosol Sci. 29 (4) (1998) 421–444, https://doi.org/10.1016/S0021-8502(98)00013-5.